

RESEARCH ARTICLE

Broadband Three-Section Branch-Line Coupler Realized by Ridge Gap Waveguide Technology From 12 to 20 GHz

PARISA MAHDAVI¹, S. ESMAIL HOSSEINI¹, (Member, IEEE), AND PEDRAM SHOJAADINI²¹Department of Communications and Electronics, School of Electrical and Computer Engineering, Shiraz University, Shiraz 71348-14336, Iran²Computer Sciences and Engineering Department, University of Quebec in Outaouais, Gatineau, QC J8X 3X7, Canada

Corresponding author: S. Esmail Hosseini (se.hosseini@shirazu.ac.ir)


ABSTRACT The novel ridge-gap waveguide (RGW) technology which uses an entire metal structure has various advantages at high frequencies, such as broad bandwidth, low loss, low sensitivity to manufacturing errors, and uncomplicated integration with passive and active components. In this paper, a broadband RGW-based three-section branch-line coupler in the frequency band of 12 to 20 GHz is proposed, simulated, and experimentally demonstrated. The proposed structure employs four short stubs at the branches with a quarter wavelength for impedance matching. Also, four steps have been added for better power division on the coupling branch lines. The proposed structure with WR62 transition shows low-loss, equal-power division, 90-degree with good impedance matching, and isolation in the frequency band of 12-20 GHz containing the Ku band, and, the measured results are in good agreement with the simulations. The introduced structure can be extended to an arbitrary broadband power divider/combiner, which can find various applications, such as in array antenna feed networks and solid-state power amplifiers. It can be redesigned for broadband, high-power, and low-cost millimeter-wave applications.

INDEX TERMS Branch-line coupler, Ku band, ridge gap waveguide (RGW), return loss, insertion loss.

I. INTRODUCTION

Branch Line Coupler is one of the substantial components in microwave engineering [1], [2]. Various types of couplers have been designed and made in different structures, such as rectangular waveguides, microstrip, substrate-integrated waveguides (SIW), and ridge gap waveguides (RGW). These structures have various applications, such as in balanced amplifiers and mixers, for obtaining good return loss and high spurious signal rejection [3]. Communication systems have recently received advantages from high-frequency bands in case of high data rates. Millimeter-wave (mm-wave) requires low transmission loss, low dispersion, uncomplicated fabrication structures, and power handling capability [4]. Therefore, there are different traditional guided structures, such as rectangular waveguides, strip-line, and microstrip transmission lines for mm-wave applications. However, in high-frequency

uses, rectangular waveguide contains manufacturing problems [5], [6], [7]. Also, significant transmission loss of strip-line, SIW, and microstrip lines has become a disadvantage in high-power and high-frequency applications. As a result, RGW had been represented to satisfy the mm-wave in high-power applications [8]. Because of quasi-TEM mode propagation in RGW, this structure has sufficient advantages, including low-signal dispersion [9]. The first appearance of RGW technology was proposed in 2009 [5]. The main idea behind RGW is the expansion of soft and hard surfaces, which was first introduced in 1988 [9], [10], [11]. This structure contained two separate conducting plates, a ridge, and a bed of nails. The bed of nails near the ridge works as an artificial magnetic conductor (AMC), intercepting wave propagation. As a result, the wave propagates in the air between the ridge and the upper plate and causes low-loss transmissions. In addition, the merits of the RGW structure, encompassing broad bandwidth, low loss, low sensitivity to fabrication error, and uncomplicated integration of active components,

The associate editor coordinating the review of this manuscript and approving it for publication was Muhammad Usman Afzal .

make it suitable for various applications [4], [5], [6], [7], [8], [9], [10], [11], [12], [13], [14], [15], [16], [17]. Recently, RGW-based components have been considered in various designs functioning as antenna array feed networks [11], couplers [13], [14], combiners [15], filters [16], [25], and power dividers [18], [19], [20].

Efforts have been made to realize couplers, especially directional and branch line couplers in the RGW platform. A directional coupler based on RGW has been designed and implemented for the frequency band of 13.5 to 16.5 GHz. The narrow bandwidth, the imbalance amplitude at the beginning of the considered frequency band, and the significant difference between the measured and simulated results, especially at the end of the frequency band, are the disadvantages of this structure [4]. Also, two other 3 dB 90-degree couplers, one branch line, and the other, coupled line directional coupler have been designed and fabricated based on RGW for the frequency band of 14-16 GHz. Unequal power split and significant phase imbalance have made these structures narrow bands [17].

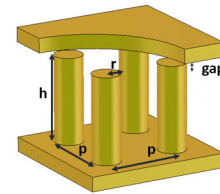
Some techniques have been used to realize the 3 dB branch-line coupler using PRGW (Printed Ridge Gap Waveguide) technology, which is considered a subset of RGW. PRGW was introduced in 2012 [27]. Various structures, such as filters, antennas, and couplers, have been designed and realized based on PRGW. A 3 dB quadrature hybrid coupler has been designed and implemented based on PRGW with a central frequency of 30 GHz and a bandwidth of 6% [8]. Using the technique of increasing the number of sections by introducing a specific boundary condition has led to the design and fabrication of a wideband dual box hybrid coupler with a bandwidth of 46% at the central frequency of 30 GHz based on PRGW [26]. In addition, an ultra-wideband four-layer compact directional coupler for 5G applications in the central frequency of 30 GHz has been designed, assembled, and tested [28]. Despite the ultra-wideband and small size being the advantages of PRGW, these structures have a considerable loss and the difficulty in assembling them leads to a significant manufacturing error and measuring deviation. The presence of a dielectric substrate restricts power tolerance in high-power applications.

In this paper, a self-packaged 3-dB branch-line coupler at the frequency range of 12-20 GHz is proposed and manufactured. Furthermore, it can be used to realize an arbitrary $1:2^N$ power divider/combiner, Butler Matrix, etc. This structure has over 50% bandwidth with the advantage of low amplitude and phase imbalance at the whole working frequency band. Also, high isolation and return loss have been achieved.

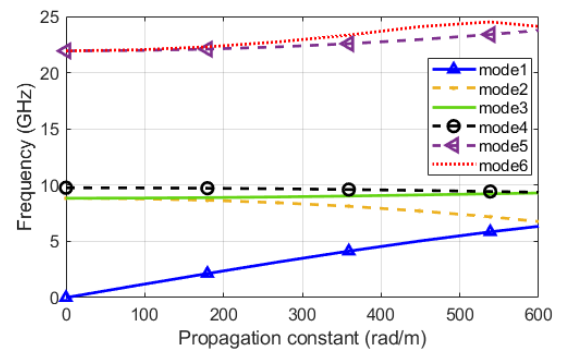
In the following, section II presents an approach for unit cell design and RGW transmission line supporting Ku-band frequency. The effect of geometric parameters on waveguide performance is investigated in section III. In section IV, the circuit model of the proposed structure is simulated using circuit simulation software, ADS. RGW-based branch-line coupler design and simulation are presented in section V.

TABLE 1. Parameters values of the designed unit cell.

Parameter	Value (mm)	Parameter	Value (mm)
r	1	h	6
p	5	gap	0.61



(a)



(b)

FIGURE 1. (a) Dimensions of the unit cell without ridge. (b) dispersion diagram of the unit cell.

For measurement with standard devices, an RGW-to-WR62 transition is designed in section VI. To validate the proposed design, the structure has been manufactured, and the results are shown in section VII.

II. RGW UNIT CELL DESIGN AND DISPERSION DIAGRAM

In this section, two steps of designing the unit cell for the proposed RGW-based branch-line coupler are presented. First, the parameters of the ridge surrounded by the periodic unit cell are calculated and simulated. Subsequently, the ridge of the structure was designed with the known unit cell dimensions in the center of the desired frequency bandwidth. In this paper, all simulation responses are obtained using CST Microwave Studio simulator.

A. UNIT CELL DESIGN AND DISPERSION DIAGRAM

The first step in presenting the proposed branch-line coupler is to design the RGW unit cell. These periodic nails act as a perfect magnetic conductor (PMC) in a narrow frequency band. Therefore, the electromagnetic wave cannot propagate in the bed of the nail structure. Essential parameters to design unit cells are illustrated in Fig. 1 (a), and the values are given in Table. 1 for the Ku band. These dimensions are used in the rest of the paper. Besides, the related dispersion diagram for the designed unit cell is shown in Fig. 1 (b). This figure shows that the unit cell stopband is from 10 GHz to 22 GHz, containing the Ku band.

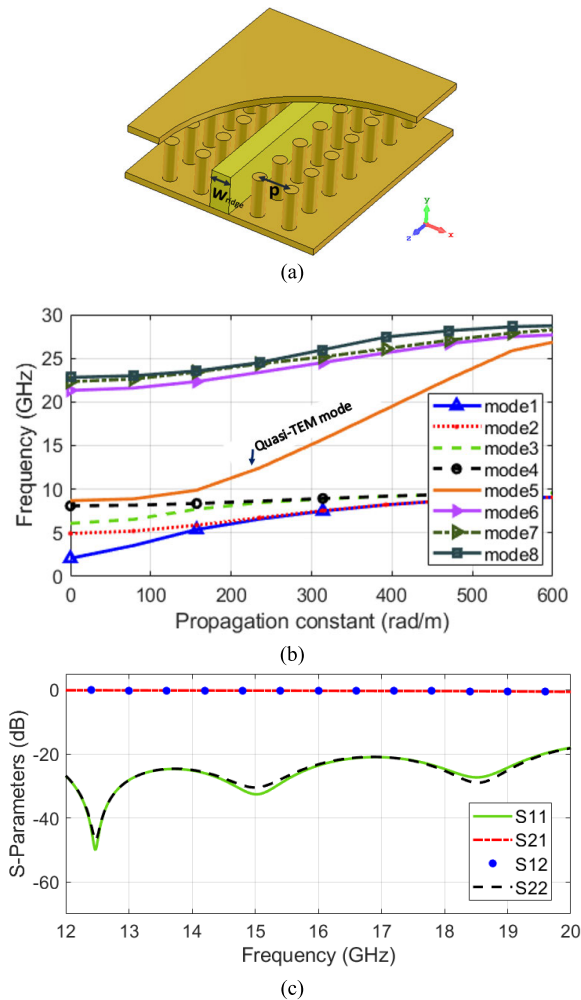


FIGURE 2. (a) Unit cell with ridge. (b) simulated dispersion diagram of the unit cell. (c) simulated S-parameters of the RGW line.

B. UNIT CELL WITH RIDGE AND DISPERSION DIAGRAM

As shown in Fig. 1 (b), the wave cannot propagate in periodic unit cells from 10 GHz to 20 GHz (stop band). Also, the approach to designing unit cells can be found in [21]. A ridge is added to the unit cell for wave propagation, which is shown in Fig. 2 (a), in which W_{Ridge} is 3.05 mm. The wave propagates in the air between the ridge and the upper plate. The dispersion diagram of the designed unit cell with a ridge is shown in Fig. 2 (b). Demonstrated, a quasi-TEM mode propagates at 10.5-22 GHz. Therefore, the operating bandwidth of the structure contains the entire Ku-band. Also, Fig. 2 (c) demonstrates the simulated S-parameters of the RGW transmission line. Return loss (S11) is mostly less than -20 dB, and S21 (transmission) is better than 0.01 dB. So, this RGW platform can be used to realize an RGW-based branch-line coupler.

III. INVESTIGATING THE EFFECT OF GEOMETRIC PARAMETERS ON WAVEGUIDE PERFORMANCE

A study has been conducted on the stop band of the gap waveguide and how the stop band changes when the effective

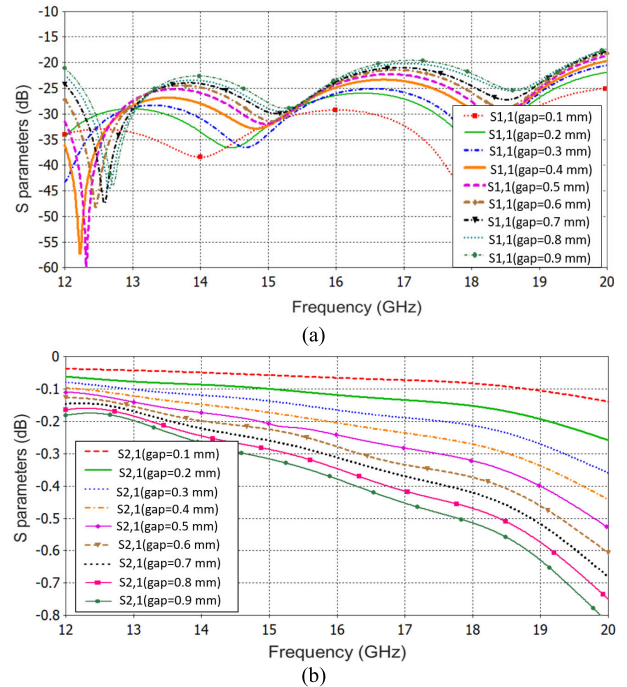


FIGURE 3. Scattering parameters for different height gaps for the RGW line in Fig. 2(a). (a) Return loss. (b) insertion loss. (The pins are circular with height $h = 6$ mm, radius $r = 1$ mm, period of the nails $p=5$ mm, and $W_{\text{Ridge}} = 3$ mm.)

parameters are varied. The parametric study of the cut-off bandwidths of three artificial surfaces has been presented, namely the bed of nails (unit cell in RGW), transverse corrugations, and mushrooms [27]. Based on the results of the RGW simulation in this study, it is possible to achieve an octave cut-off bandwidth using a bed of nails. Besides, the parameters of an RGW unit cell have been studied as a coefficient of the wavelength corresponding to the central frequency [12]. However, this section discusses the effect of geometrical parameters affecting the performance of the RGW line. For this purpose, scattering parameters and line impedance in the states of gap and ridge width changes have been obtained using CST full-wave software.

A. INVESTIGATING THE PERFORMANCE CHANGES OF THE RGW LINE BY CHANGING THE VALUE OF THE AIR GAP

Fig. 3 (a) indicates the changes in the return loss compared to the gap changes. In this figure, it can be seen that S_{11} parameter decreases as the gap decreases. Also, the changes in the insertion loss with the changes in the gap are shown in Fig. 3 (b), which shows the improvement of the S21 parameter and the reduction of the transmission loss with the reduction of the gap. These changes are shown in Fig. 4 (a) and (b) as a function of the return loss/gap and insertion loss/gap for the center frequency of 16 GHz, respectively. The pins are cylindrical with the radius $r=1$ mm, the height is $h = 6$ mm, the period of the nails is $p=5$ mm and the width of the ridge is $W=3$ mm. According to Fig. 4 (a) and (b), the return loss

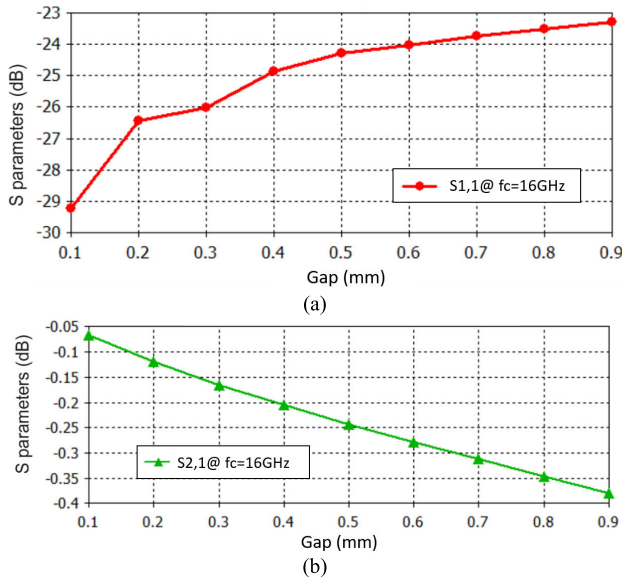


FIGURE 4. (a) Return loss. (b) Insertion loss as a function of height gap for the RGW line in Fig. 2(a). (The pins are circular with height $h = 6$ mm, radius $r = 1$ mm, period of the nails $p=5$ mm, and $W_{Ridge} = 3$ mm.)

and the transmission loss increase with the increase of the gap value. But according to these two investigations, it cannot be concluded that less gap is chosen for the design of the coupler structure, and what is important and should be focused on is the value of line impedance and its realization in practice. For this purpose, line impedance changes compared to gap changes are simulated and shown in Fig. 5 (a). It can be clearly seen that the impedance increases as the gap increases. This diagram shows that to realize the impedance of 50 Ohms, the proportional gap is about 0.6 mm. Impedance variation with gap change is shown as a function of impedance/gap for different gaps for a center frequency of 16 GHz in Fig. 5 (b). It can be easily seen that as the gap increases, the impedance increases, and the gap trend is upward.

B. EXAMINING THE PERFORMANCE CHANGES OF THE RGW LINE BY CHANGING THE LINE WIDTH VALUE

Another parameter that affects the performance of RGW is the width of the ridge. Variations of scattering parameters, return loss, and transmission loss are shown in Fig. 6 (a) and (b), respectively. Fig. 6 (a) demonstrates the changes of the S11 parameter with the change of ridge width, showing the reduction of return loss by increasing the width of the ridge, and assuming that other parameters are kept constant. The pins are cylindrical with a radius $r=1$ mm, the gap height is $gap=0.61$ mm, the period of the nails is $p=5$ mm and the height of the pins is $h=6$ mm. While Fig. 6 (b) shows the transmission loss that decreases with the increase of the width of the ridge. Fig. 7 (a) and (b) indicate the changes of these two parameters as a function of the return loss/width and insertion loss/ width of the ridge for the center frequency of 16 GHz, respectively, which shows that the changes of S11

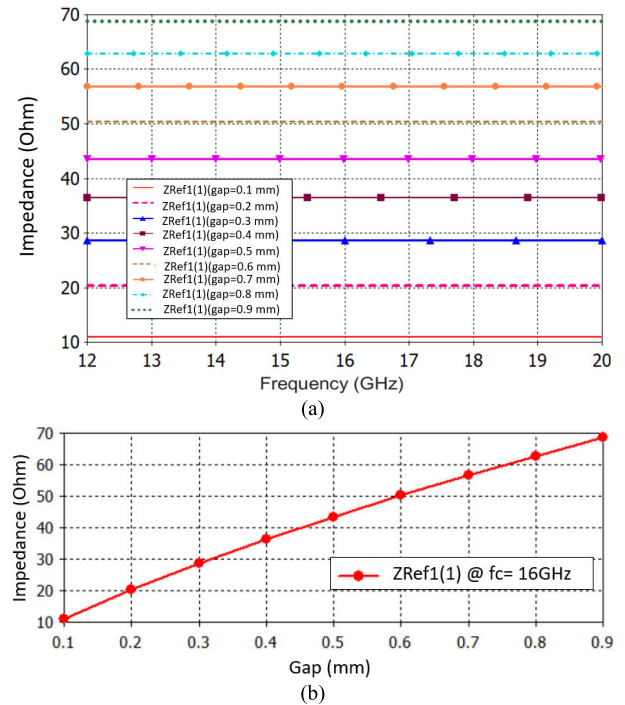


FIGURE 5. (a) Reference impedance for different height gaps. (b) Reference impedance as a function of height gap for the RGW line in Fig. 2(a). (The pins are circular with height $h = 6$ mm, radius $r = 1$ mm, period of the nails $p=5$ mm, and $W_{Ridge} = 3$ mm.)

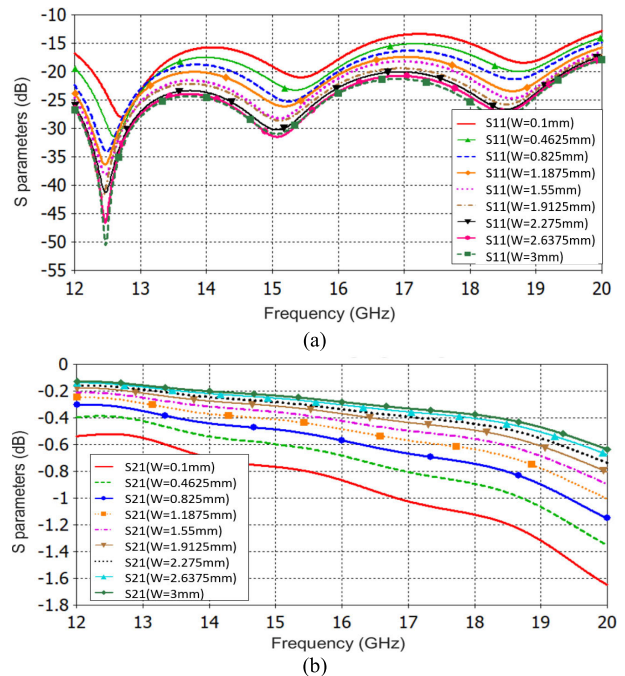


FIGURE 6. Scattering parameters for different widths of the ridge for the RGW line in Fig. 2(a). (a) Return loss. (b) insertion loss. (The pins are circular with height $h = 6$ mm, radius $r = 1$ mm, period of the nails $p=5$ mm, and gap height $gap= 0.66$ mm.)

and S21 are downward and upward respectively regarding the increase of the ridge width, but as mentioned earlier, what

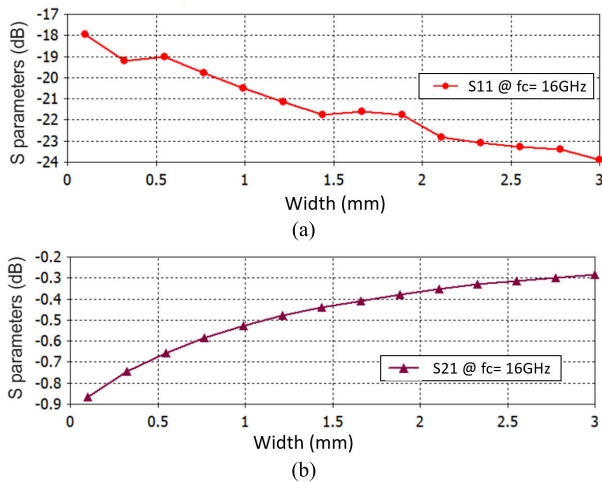


FIGURE 7. (a) Return loss. (b) Insertion loss as a function of width of the ridge for the RGW line in Fig. 2(a). (The pins are circular with height $h = 6$ mm, radius $r = 1$ mm, period of the nails $p=5$ mm, and gap height $gap = 0.66$ mm.)

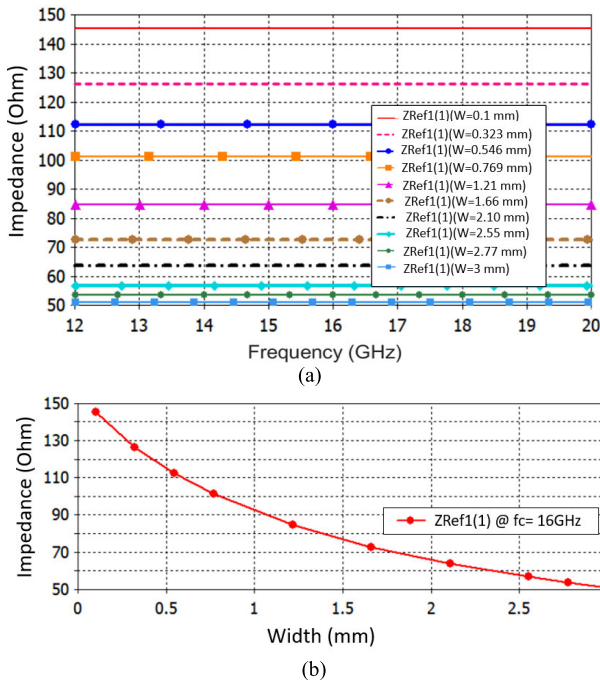


FIGURE 8. (a) Reference impedance for different widths of the ridge. (b) Reference impedance as a function of widths of the ridge for the RGW line in Fig. 2(a). (The pins are circular with height $h = 6$ mm, radius $r = 1$ mm, period of the nails $p=5$ mm, and gap height $gap = 0.66$ mm.)

is more important for designing RGW-based devices, is the line impedance. The line impedance changes compared to the ridge width changes are shown in Fig. 8 (a), which indicates the decrease in line impedance with increasing ridge width. Fig. 8 (b) shows impedance variation with ridge width change at the central frequency of 16 GHz. It can be easily seen that as the width increases, the impedance decreases and the graph trend is downward.

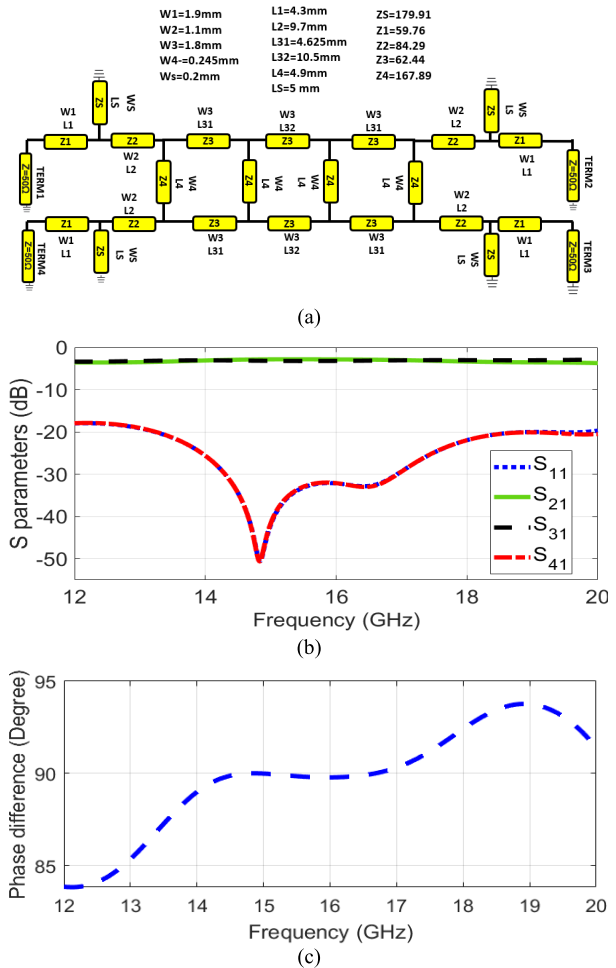


FIGURE 9. (a) Schematic of the stripline circuit model of the three-section branch-line coupler. (b) simulated S-parameters (ADS Software). (c) phase difference of the two outputs.

IV. MODELING BRANCH-LINE COUPLER IN STRIPLINE

In this section, the stripline model of the proposed RGW-based three-section branch-line coupler is obtained. To have a faster approach to finding the approximate impedance of RGW branches, this structure is simulated as a stripline model using circuit simulation software, ADS. First, according to the operating frequency and assuming the initial value of the λ of the central frequency as a coefficient of the lengths and, the impedances of the ideal branch line coupler, the prototype structure of the three-section branch line coupler is designed [2]. To increase the bandwidth, four $\lambda/4$ shorted stub connection has been added [29]. In this simulation, the characteristics of the substrate include a height of 0.5 mm, $\epsilon_r = 1$, and $\mu_r=1$. Then, optimization is performed using Advanced Design System (ADS) circuit simulator with the goals being $|S_{11}| \leq -15$, $|S_{21}|$, $|S_{31}| = -3$ and $\angle S_{21} - \angle S_{31} = 90^\circ$. The new impedances after optimization and the calculated widths corresponding to the impedance of each branch using the line calculator in ADS software are shown in Table. 2 and Fig. 9 (a). Second, the impedances of the branches in the

TABLE 2. Impedances and corresponding widths of the branches in the circuit simulation.

Parameter	Impedance (ohm)	Parameter	Width (mm)
Z1	59.76	W1	1.9
Z2	84.29	W2	1.1
Z3	62.44	W3	1.8
Z4	167.89	W4	0.245
Zs	179.91	Ws	0.2

stripline platform are converted to the impedances of the branches in the RGW.

The relation between the characteristic impedance of an ideal gap waveguide and strip line is [12]:

$$Z_{Gapwaveguide} = 2Z_{Stripline} \tag{1}$$

where $Z_{Stripline}$ is defined as [12]:

$$Z_{Stripline} = (\eta/4)(We/2h + 0.441)^{-1} \tag{2}$$

With [12]:

$$\frac{We}{2h} = \frac{We}{2h} - \begin{cases} 0 & , \frac{W}{2h} > 0.35 \\ (0.35 - (\frac{W}{2h})^2) & , \frac{W}{2h} < 0.35 \end{cases} \tag{3}$$

Although this is a fast estimate formula for obtaining characteristic impedance, it is not accurate enough, and values in RGW design must be optimized. The circuit schematic of the structure is shown in Fig. 9 (a). The stubs have been added to the schematic for impedance matching of the branch lines. As mentioned, it should be notable that the impedance of the first model is optimized for achieving a wideband coupler with better flatness for transmission and more isolation in the isolated port. Simulated S-parameters of the circuit model are shown in Fig. 9 (b). As shown, S11 (return loss) is less than -18 dB, and S21 (transmission) flatness is better than 1 dB in the desired frequency band. Besides, Fig. 9 (c) shows the phase difference between the two output ports (transmission and coupling). The phase difference ($\angle S21 - \angle S31$) is 90 degrees, with almost 4 degrees of ripple. The length of the branches and the short-circuited branch are almost $\lambda/4$ [29]. Using (1), (2), and (3), the impedance of the branches is calculated. Then, based on the impedances obtained for each branch, and using the unit cell and RGW line in section II, the dimensions of the branches are obtained using CST software. As mentioned before, these converted values are inaccurate and must be optimized in a full-wave simulation. In the following, this structure is simulated in RGW technology.

V. RGW-BASED BRANCH-LINE COUPLER DESIGN

Using the designed RGW structure in section II and the calculated impedances in section III, an RGW-based three-section branch-line coupler is realized, as shown in Fig. 10 (a). Fig. 10 (b) shows the perspective view of the structure. Fig. 10 (b') and 10 (b'') show the zoomed shorted branch and small step, respectively. Simulation results are shown in

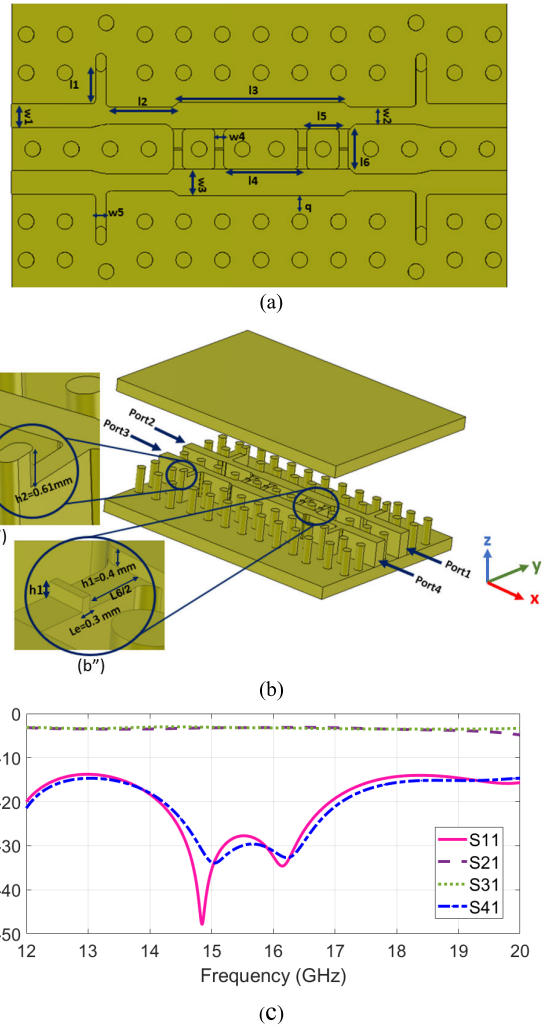


FIGURE 10. (a) Designed RGW-based three-section branch-line coupler. (b) Perspective view ((b') Shorted matching branch, (b'') Small step). (c) Simulated s-parameters of the structure.

Fig. 10 (c); transmission and coupling (S21, S31) is about -3 dB in the frequency band of 12-20 GHz, so the input power splits equally between two output ports. Also, the power imbalance (S21-S31) is less than 0.5 dB. The isolation between input and output ports (S41) is better than -15 dB, and the return loss (S11) is better than -14 dB. It should be noted that the considered material for structures is aluminum in simulations. As mentioned, all structures are simulated in CST full wave analysis software.

A. EFFECT OF THE SMALL STEP ON THE RIDGE ON THE PERFORMANCE

The influence of the small step on the middle ridges will be discussed. Fig. 10 (b'') shows these steps and values (Le and h1 are the widths and the height of the step, respectively). This small step works as line impedance tuning. In this tuning method, two adjustable parameters are the step dimensions; width and height. Fig. 11 (a) and (b) show the changes in the magnitude difference (S21(transmission)-S31(coupling))

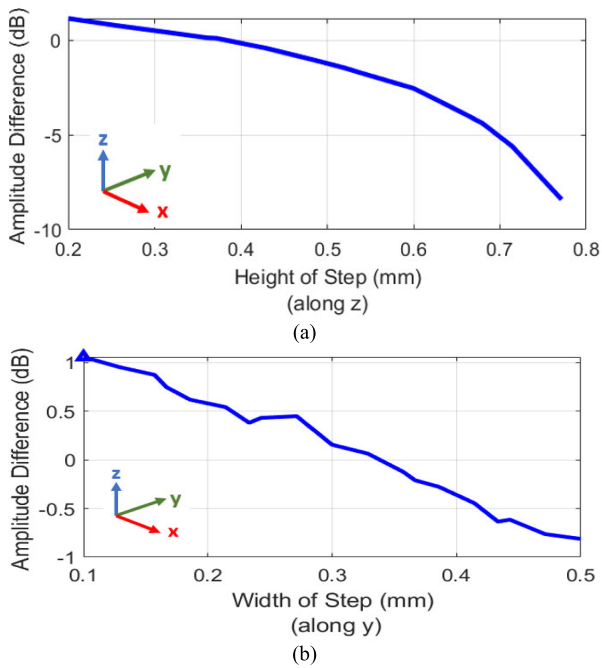


FIGURE 11. (a) Changes in amplitude difference with the step height. (b) Changes in amplitude difference with the step width.

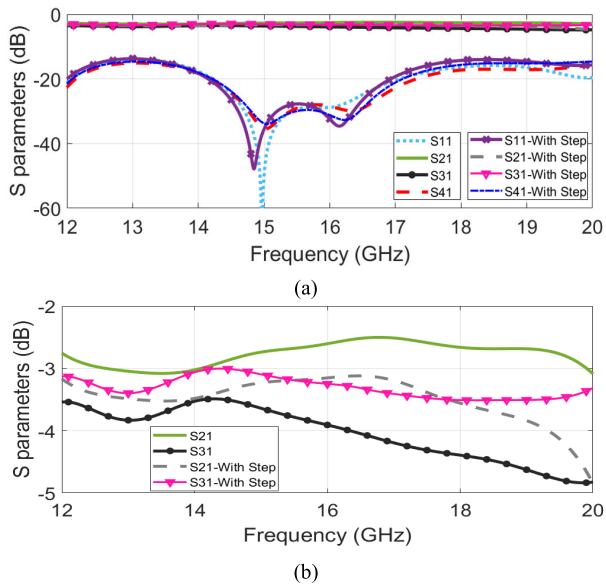


FIGURE 12. (a) S parameters of the structure with and without steps on the middle ridges. (b) transmission (S21) and coupling (S31) with and without steps on the ridges.

in two output ports with the changes in the height (when the width is constant and equals 0.3 mm) and width of the step (when the height is constant and equals 0.36 mm) at the frequency of 16 GHz, respectively. The width and height of this step affect the change of power splitting.

According to Fig. 11 (a) and (b), the difference between the values of the outputs at the frequency of 16 GHz is zero when the width of the step is $L_e = 0.38$ mm, and

TABLE 3. Optimized dimension values of the RGW-to-WR62 transition.

Parameter	Value (mm)	Parameter	Value (mm)
d1	1.44	m1	6.72
d2	2.33	m2	4.77
d3	0.92	m3	2.55
d4	0.51	m4	2.57
d5	0.45	m5	4.52
d6	1.24	l7	37.44

TABLE 4. Optimized parameters of the designed branch-line coupler.

Parameter	Value(mm)	Parameter	Value (mm)
l1	4.4	w1	3.05
l2	7.51	w2	2.22
l3	20.95	w3	3.5
l4	8.55	w4	1.14
l5	3.17	w5	1.36
l6	4.2	q	2.82

its height is $h_1=0.4$ mm. These values have been obtained by sweeping the width and height of the step, as well as by using optimization in CST software to find the best response of S parameters, especially coupling, and transmission. Fig. 12 (a) and (b) show the S parameters and the difference between coupling and transmission in two cases, one with the step on the ridge and the other without the step, respectively. according to Fig.12 (a), steps do not make significant changes in return loss and isolation (S11 and S41) while based on Fig. 12 (b) with the step (if $L_e = 0.38$ mm and $h_1=0.4$ mm), the difference between two parameters, coupling, and transmission, is about 1 dB better than when the step doesn't exist. Step improves and, more precisely, adjusts the impedance in the entire frequency range.

B. EFFECT OF THE SHORTED $\lambda/4$ STUBS

The effect of shortened stubs on the S parameters of the structure has been investigated. Analysis of the impact of shortened connection stubs has been studied in [29]. Fig. 13 (a) shows the S parameters in two cases; with four $\lambda/4$ stubs shortened and without these stubs. It can be seen that the return loss and isolation parameters have been significantly improved when stubs exist. The realization of stub shorting in RGW technology is to connect the end of the stub to the upper plate. Fig. 13 (b) shows the insertion loss and transmission in the case with the shortened stub and without it. It can be seen that the shortened stubs have improved the mentioned parameters to some extent. The design procedure for the proposed branch line coupler can be described as demonstrated in Fig. 14.

VI. RGW-TO-WR62 TRANSITION

For the measurement of the proposed RGW-based structure with standard connectors, the transition of RGW to

TABLE 5. Comparison with some similar branch line couplers in different structure.

Ref.	Technology	Center frequency (GHz)	Bandwidth (S11<-10 dB)	Amplitude Balance (dB) BW% (imbalance < 2 dB)	Phase impedance BW% (imbalance < 5°)	substrate
[4]	RGW	15.5	14%	-3 ±0.5 BW= 7%	Not reported	no
[6]	PRGW	30	26.5%	3.7±0.75 BW= 6%	90±5 BW= 6%	yes
[8]	PRGW	30	6%	-3.6±1 BW= 6%	90±10 BW= 6%	yes
[17]	RGW	15	3%	-7.5±3.75 BW=3%	85±4 BW=3%	no
[30]	Microstrip	30	11%	-4±1 BW= 11%	90±1 BW= 11%	yes
[31]	PRGW	60	11%	-3.7±0.5 BW= 11%	90±5 BW= 11%	no
[32]	PRGW	30	13%	-3.6±0.5 BW= 6.7%	90±10 BW=14%	yes
[33]	RGW	11	13%	-3±1 BW= 9%	89±5 BW= 9.3%	no
[34]	SIW	24	18%	4.7±0.5 BW=10%	92±2 BW= 18%	yes
[35]	PRGW	30	26.6%	3.6±0.75 13%	90±5 BW= 26.5%	yes
This work	RGW	16	50%	-3 ±0.7 50%	91±3 BW= 50%	no

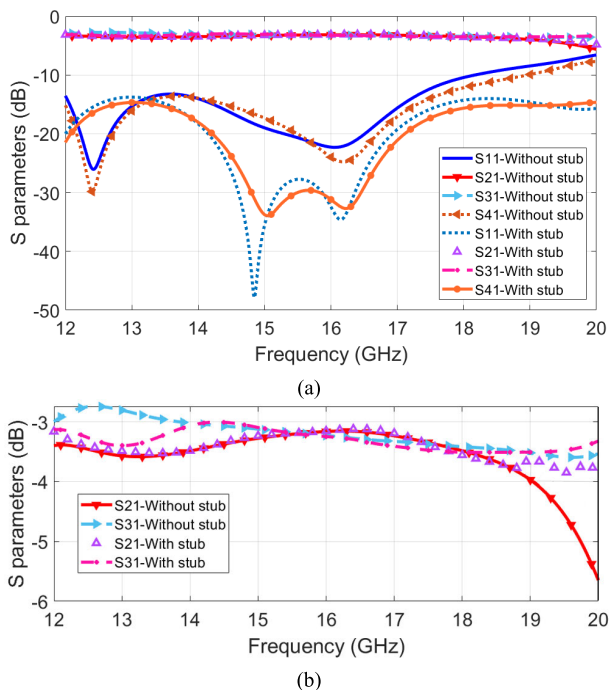


FIGURE 13. (a) S parameters of the structure with and without four $\lambda/4$ stubs. (b) Amplitudes of the structure with and without four $\lambda/4$ stubs.

a rectangular waveguide or coaxial connectors is required. Several RGW to other standard ports has already been designed, such as coaxial, microstrip lines, and rectangular waveguides [22]. RGW-to-rectangular waveguide transition has already been presented in two types, vertical and

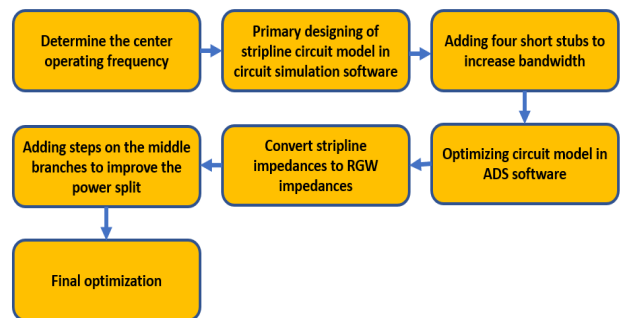


FIGURE 14. Block diagram for the design and process of the branch line coupler.

horizontal [23], [24]. In the Ku band, the standard rectangular waveguide is WR62.

In this section, an RGW-to-WR62 transition has been designed. The proposed transition is shown in Fig. 15 (a) and (b), with the parameters' values in Table. 3. Simulation results of the transition are shown in Fig. 15 (c). Transmission and return loss is better than 0.05 dB and -23 dB, respectively, in the desired frequency band. For measurement, the RGW-based structure will be fed with a coaxial port. This structure should be connected to the standard waveguide WR62 for the desired frequency band for practical use. Using the designed RGW-to-WR62 transitions in section V, the proposed RGW-based three-section branch-line coupler with transitions is shown in Fig. 16. Table. 4 shows the optimized values of the dimensions for the final structure. Simulated S-parameters of the structure are shown

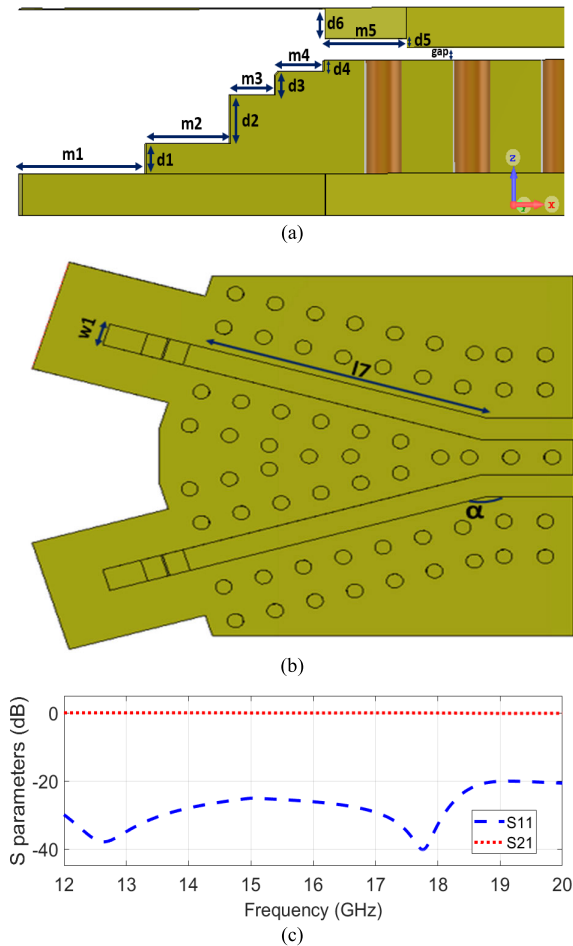


FIGURE 15. RGW-to-WR62 transition, (a) Side view. (b) Top view of the designed structure. (c) Simulated S-parameters

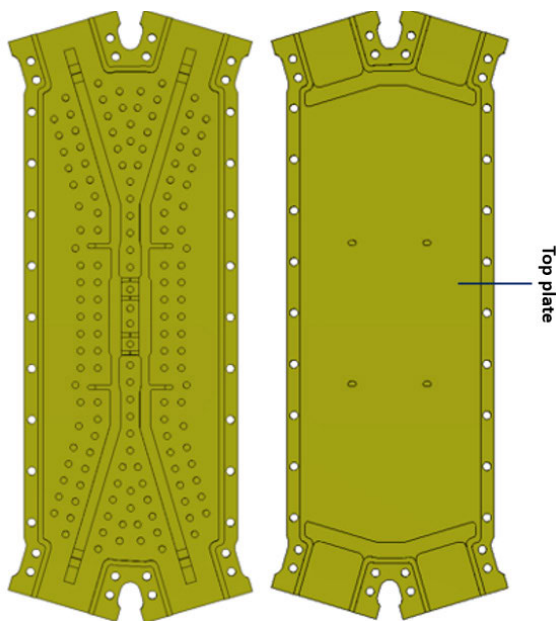


FIGURE 16. Designed RGW-based three-section branch-line coupler with RGW-to-WR62 transitions.

in Fig. 17 (a). Magnitudes, the difference between coupling and transmission, and the phase difference are shown in

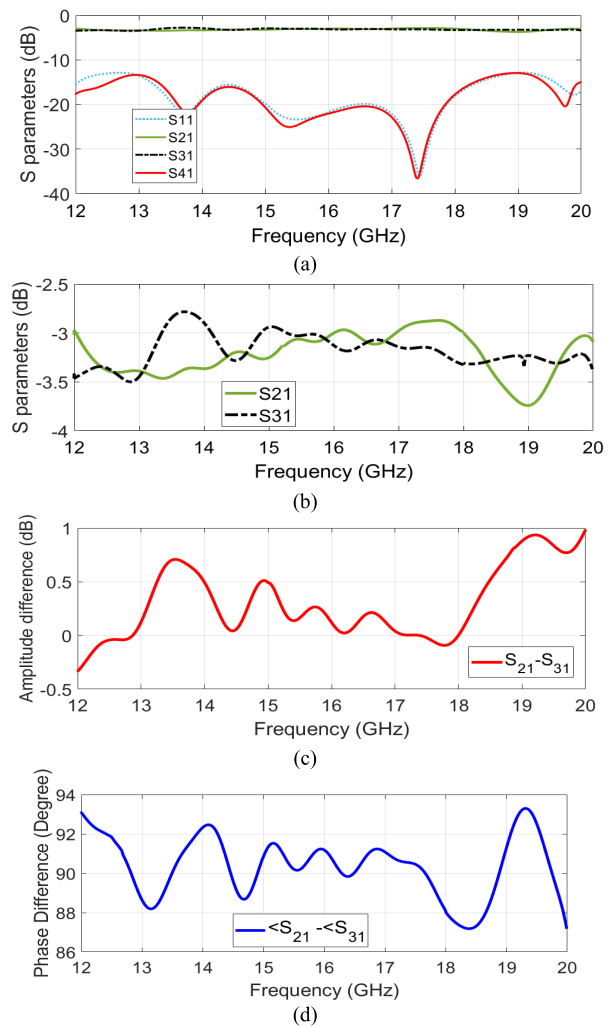


FIGURE 17. (a) Simulated S-parameters of the structure. (b) Amplitudes. (c) Amplitude difference. (d) Phase difference of the two output ports.

Fig. 17 (b), (c), and (d), respectively. Return loss and isolation are better than -14 dB, and transmission is about -3 dB at the frequency band of 12-20 GHz. Besides, Fig. 17 (d) shows the phase difference between the two output ports. The phase difference ($\angle S_{21} - \angle S_{31}$) is 90 ± 3 degrees in the frequency range of 12-20 GHz.

VII. EXPERIMENTAL RESULTS

The designed RGW-based three-section branch-line coupler with RGW-to-WR62 transitions was fabricated and shown in Fig. 18 (a). This structure was manufactured using aluminum machining. The scattering parameters have been measured using a vector network analyzer (VNA). TRL (thru-reflect-line) calibration has been used to de-embed the impact end launch connectors and transitions in measurements since a rectangular coax-to-WR62 waveguide converter was used. Measured S-parameters, and the setup is shown in Fig. 18 (b). Measured return loss, transmission, coupling, and isolation are shown in Fig. 19 (a) and (b), compared with simulation

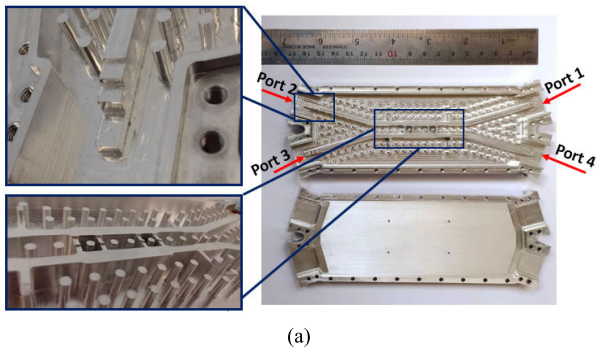


FIGURE 18. (a) Fabricated RGW-based three-section branch-line coupler, and (b) measurement setup.

results. Based on this figure, measured return loss and isolation are mostly less than -14 dB, which is in good agreement with simulations. It should be mentioned that the measured transmission is about 0.7 dB less than the simulations. This transmission loss is due to using a coaxial-to-waveguide converter. Also simulated and measured magnitude difference is shown in Fig. 19 (c). In addition, the measured phase difference between the two output ports is shown in Fig. 19 (d), which is compared with simulation results; the measured phase difference of the output ports is about 90 ± 3 degrees in most of the desired frequency band. It should be mentioned that the difference between simulated and measured results is because of the inaccuracy of manufacturing roughness, which can be decreased by improving manufacturing accuracy. To evaluate the performance of the proposed coupler and compare it with the performed works, Table. 5 is presented. In this table, branch line coupler structures realized using different guiding structures, which are promising technologies for millimeter wave applications, are given. In particular, the bandwidth, phase, amplitude imbalance,

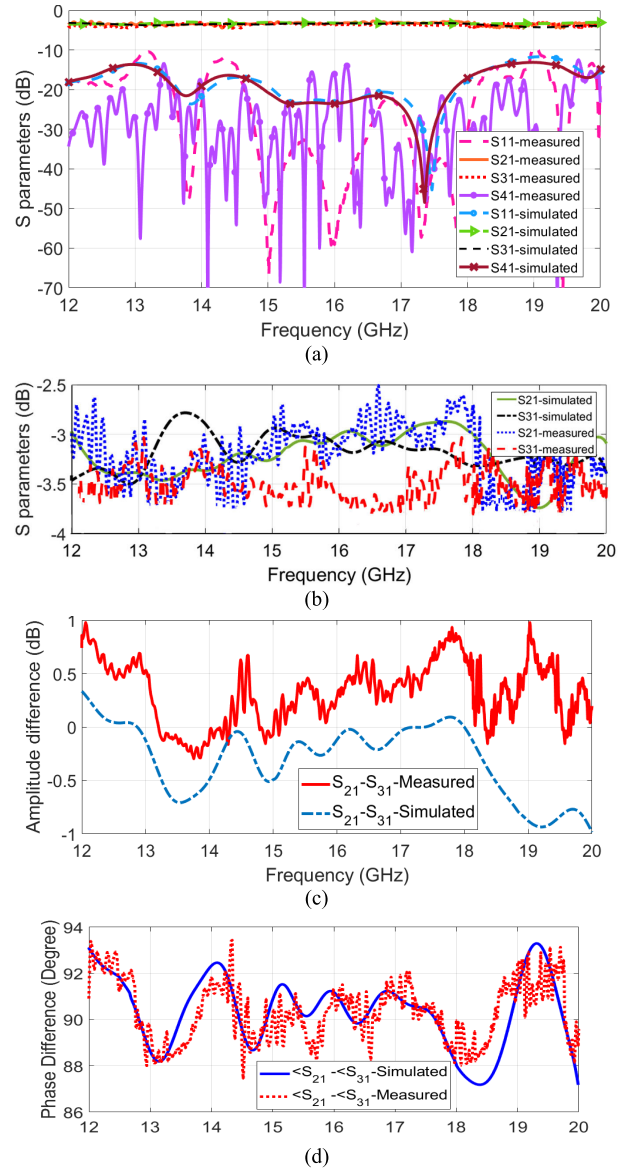


FIGURE 19. Simulated and measured results of the RGW-based three-section branch-line coupler with RGW-to-WR62 transitions (a) return loss (S11), transmission (S21), coupling (S31), and isolation (S41). (b) Amplitudes (S21 and S31). (c) Amplitude difference. (d) phase difference of the two outputs (CST software and measured).

and the use or non-use of the substrate are reported in this table. The bandwidth of the device; the frequency interval that the input matching port and isolation are better than 10 dB, is considered. In addition, the maximum amplitude imbalance and phase imbalance to obtain the amplitude and phase balance bandwidth are 2 dB and 5 degrees of tolerance, respectively. Although the proposed coupler presents a wide bandwidth with amplitude and phase imbalance less than 0.7 dB and 3 degrees, the value of 2 dB and 5 degrees is chosen according to most of the cited literature. Most of the 3 dB 90 -degree couplers in the literature have a narrow bandwidth of up to 18% of the high amplitude and phase imbalance of the output [4], [8], [17], [30], [31], [32], [33],

and [34]. The proposed couplers in [6] and [35] have more bandwidth of 26%, and 26.5%, respectively, which not only suffer from amplitude and phase imbalance but also these two structures have dielectric substrates that can limit to tolerate the power in high frequencies. Although the bandwidth in these two structures is more than the other compared references, because of the multilayered; their amplitude and phase balance bandwidth is reduced. Especially, the 3 dB 90-degree coupler structures realized in RGW technology in [4], [17], and [33], compared to the proposed work, suffer from a lower bandwidth of 14%, 3%, and 13%, respectively, and high phase imbalance and output amplitude. The proposed coupler provides 50% bandwidth and amplitude and phase balance with a maximum tolerance of 0.7 dB and 4 degrees, without using a dielectric substrate and electrical contact. The only drawback of this work is its relatively large size, $2.2\lambda \times 1.7\lambda$; because the main purpose of this work is to increase the bandwidth of the 3 dB 90-degree coupler based on RGW, the optimization to reduce the size has not been done.

VIII. CONCLUSION

In this paper, an RGW-based three-section 90-degree branch-line coupler with shorted quarter-wavelength stubs and RGW-to-WR62 transitions was presented, designed, simulated, and fabricated for the first time to the best of our knowledge. By using shorted stubs in the structure, impedance matching was improved, and reflection was reduced. Also, for the first time, the step tuners were designed on the coupling branches to improve the power splitting in this structure.

REFERENCES

- [1] S. A. Imam, A. M. Zaidi, A. Choudhary, B. K. Kanaujia, and M. K. Singh, "A quad band quadrature branch line coupler using coupled line sections," in *Proc. 2nd IEEE Int. Conf. Integr. Circuits Microsyst. (ICICM)*, Nov. 2017, pp. 120–123.
- [2] D. M. Pozar, *Microwave Engineering*. New York, NY, USA: Wiley, 2005.
- [3] M. M. M. Ali and A. Sebak, "Compact printed ridge gap waveguide crossover for future 5G wireless communication system," *IEEE Microw. Wireless Compon. Lett.*, vol. 28, no. 7, pp. 549–551, Jul. 2018.
- [4] S. I. Shams and A. A. Kishk, "Design of 3-dB hybrid coupler based on RGW technology," *IEEE Trans. Microw. Theory Techn.*, vol. 65, no. 10, pp. 3849–3855, Oct. 2017.
- [5] P.-S. Kildal, E. Alfonso, A. Valero-Nogueira, and E. Rajo-Iglesias, "Local metamaterial-based waveguides in gaps between parallel metal plates," *IEEE Antennas Wireless Propag. Lett.*, vol. 8, pp. 84–87, 2009.
- [6] M. M. M. Ali, S. I. Shams, and A. Sebak, "Ultra-wideband printed ridge gap waveguide hybrid directional coupler for millimetre wave applications," *IET Microw., Antennas Propag.*, vol. 13, no. 8, pp. 1181–1187, Jul. 2019.
- [7] A. Doghri, T. Djerafi, A. Ghiotto, and K. Wu, "Substrate integrated waveguide directional couplers for compact three-dimensional integrated circuits," *IEEE Trans. Microw. Theory Techn.*, vol. 63, no. 1, pp. 209–221, Jan. 2015.
- [8] M. M. M. Ali, S. I. Shams, and A. Sebak, "Printed ridge gap waveguide 3-dB coupler: Analysis and design procedure," *IEEE Access*, vol. 6, pp. 8501–8509, 2018.
- [9] D. Shen, K. Wang, and X. Zhang, "A substrate integrated gap waveguide based wideband 3-dB coupler for 5G applications," *IEEE Access*, vol. 6, pp. 66798–66806, 2018.
- [10] M. S. Sorkherizi, A. Khaleghi, and P.-S. Kildal, "Direct-coupled cavity filter in ridge gap waveguide," *IEEE Trans. Compon., Packag., Manuf. Technol.*, vol. 4, no. 3, pp. 490–495, Mar. 2014.
- [11] M. Al Sharkawy and A. A. Kishk, "Long slots array antenna based on ridge gap waveguide technology," *IEEE Trans. Antennas Propag.*, vol. 62, no. 10, pp. 5399–5403, Oct. 2014.
- [12] P. Kildal, A. Zaman, E. Rajo-Iglesias, E. Alfonso, and A. Valero-Nogueira, "Design and experimental verification of ridge gap waveguide in bed of nails for parallel-plate mode suppression," *IET Microw., Antennas Propag.*, vol. 5, no. 3, pp. 262–270, Feb. 2011.
- [13] A. Beltayib and A. Sebak, "Analytical design procedure for forward wave couplers in RGW technology based on hybrid PEC/PMC waveguide model," *IEEE Access*, vol. 7, pp. 119319–119331, 2019.
- [14] P. Mahdavi and S. E. Hosseini, "Ku-band two-section branch-line coupler based on ridge gap waveguide technology," in *Proc. 28th Iranian Conf. Electr. Eng. (ICEE)*, Aug. 2020, pp. 1–5.
- [15] M. M. Fahmi, J. A. Ruiz-Cruz, and R. R. Mansour, "Compact ridge waveguide Gysel combiners for high-power applications," *IEEE Trans. Microw. Theory Techn.*, vol. 67, no. 3, pp. 968–977, Mar. 2019.
- [16] B. Ahmadi and A. Banai, "Direct coupled resonator filters realized by gap waveguide technology," *IEEE Trans. Microw. Theory Techn.*, vol. 63, no. 10, pp. 3445–3452, Oct. 2015.
- [17] E. Alfonso, M. Baquero, P. Kildal, A. Valero-Nogueira, E. Rajo-Iglesias, and J. I. Herranz, "Design of microwave circuits in ridge-gap waveguide technology," in *IEEE MTT-S Int. Microw. Symp. Dig.*, May 2010, pp. 1544–1547.
- [18] A. K. Nobandegani and S. E. Hosseini, "Gysel power divider realized by ridge gap waveguide technology," *IEEE Access*, vol. 9, pp. 72103–72110, 2021.
- [19] S. E. Hosseini, M. Amrollahzadeh, and F. Ahmadfard, "A novel two-way Gysel power divider based on ridge-gap waveguide technology," in *Proc. 6th Iranian Conf. Radar Surveill. Syst.*, Dec. 2019, pp. 1–4.
- [20] A. K. Nobandegani and S. E. Hosseini, "Ku-band 8-way Wilkinson power divider based on ridge gap waveguide technology," *J. Electromagn. Waves Appl.*, vol. 35, no. 17, pp. 2283–2303, Nov. 2021.
- [21] A. Polemi, S. Maci, and P.-S. Kildal, "Dispersion characteristics of a metamaterial-based parallel-plate ridge gap waveguide realized by bed of nails," *IEEE Trans. Antennas Propag.*, vol. 59, no. 3, pp. 904–913, Mar. 2011.
- [22] S. I. Shams and A. A. Kishk, "Wideband coaxial to ridge gap waveguide transition," *IEEE Trans. Microw. Theory Techn.*, vol. 64, no. 12, pp. 4117–4125, Dec. 2016.
- [23] B. Ahmadi and A. Banai, "Substrateless amplifier module realized by ridge gap waveguide technology for millimeter-wave applications," *IEEE Trans. Microw. Theory Techn.*, vol. 64, no. 11, pp. 3623–3630, Nov. 2016.
- [24] J. Liu, A. Vosoogh, A. U. Zaman, and J. Yang, "A slot array antenna with single-layered corporate-feed based on ridge gap waveguide in the 60 GHz band," *IEEE Trans. Antennas Propag.*, vol. 67, no. 3, pp. 1650–1658, Mar. 2019.
- [25] E. Alfonso, A. U. Zaman, E. Pucci, and P. S. Kildal, "Gap waveguide components for millimeter-wave system: Couplers, filters, antenna, MMIC and packaging," in *Proc. Int. Symp. Antennas Propag. (ISAP)*, Oct. 2012, pp. 243–246.
- [26] Z. Mousavirazi, M. M. M. Ali, H. N. Gheisanab, and T. A. Denidni, "Analysis and design of ultra-wideband PRGW hybrid coupler using PEC/PMC waveguide model," *Sci. Rep.*, vol. 12, no. 1, Aug. 2022, Art. no. 14214.
- [27] E. Rajo-Iglesias and P.-S. Kildal, "Numerical studies of bandwidth of parallel-plate cut-off realised by a bed of nails, corrugations and mushroom-type electromagnetic bandgap for use in gap waveguides," *IET Microw., Antennas Propag.*, vol. 5, no. 3, p. 282, 2011.
- [28] M. M. M. Ali, O. M. Haraz, I. Afifi, A.-R. Sebak, and T. A. Denidni, "Ultra-wideband compact millimeter-wave printed ridge gap waveguide directional couplers for 5G applications," *IEEE Access*, vol. 10, pp. 90706–90714, 2022.
- [29] G. P. Riblet, "A directional coupler with very flat coupling," *IEEE Trans. Microw. Theory Techn.*, vol. MTT-26, no. 2, pp. 70–74, Feb. 1978.
- [30] X. F. Ye, S. Y. Zheng, and Y. M. Pan, "A compact millimeter-wave patch quadrature coupler with a wide range of coupling coefficients," *IEEE Microw. Wireless Compon. Lett.*, vol. 26, no. 3, pp. 165–167, Mar. 2016.
- [31] M. Farahani, M. Akbari, M. Nedil, T. A. Denidni, and A. R. Sebak, "A novel low-loss millimeter-wave 3-dB 90° ridge-gap coupler using large aperture progressive phase compensation," *IEEE Access*, vol. 5, pp. 9610–9618, 2017.
- [32] Z. Zhao and T. A. Denidni, "Millimeter-wave printed-RGW hybrid coupler with symmetrical square feed," *IEEE Microw. Wireless Compon. Lett.*, vol. 30, no. 2, pp. 156–159, Feb. 2020.

- [33] M. Taraji and M. Naser-Moghaddasi, "Design of branch line coupler based on ridge gap waveguide technology for X-band application," *IETE J. Res.*, vol. 68, no. 2, pp. 917–923, Mar. 2022.
- [34] T. Djerafi and K. Wu, "Super-compact substrate integrated waveguide cruciform directional coupler," *IEEE Microw. Wireless Compon. Lett.*, vol. 17, no. 11, pp. 757–759, Nov. 2007.
- [35] M. M. M. Ali, M. S. El-Gendy, M. Al-Hasan, I. B. Mabrouk, A. Sebak, and T. A. Denidni, "A systematic design of a compact wideband hybrid directional coupler based on printed RGW technology," *IEEE Access*, vol. 9, pp. 56765–56772, 2021.



PARISA MAHDAVI received the B.Sc. degree in electrical engineering from the Shahid Bahonar University of Kerman, in 2016, and the M.Sc. degree in electrical engineering from Shiraz University, Shiraz, Iran, in 2020. During the master's degree, she worked on the design and simulation of microwave couplers, power dividers/combiners, and antennas. In particular, she studied multi-output couplers based on ridge gap waveguide (RGW) technology in Ku band. Her research interests include antennas and microwaves/millimeter-waves.



S. ESMAIL HOSSEINI (Member, IEEE) received the B.Sc. degree in electrical engineering from Shiraz University, Shiraz, Iran, in 2007, and the M.Sc. and Ph.D. degrees in electrical engineering (microwave and optical communications) from the Sharif University of Technology (SUT), Tehran, Iran, in 2009 and 2014, respectively. From 2013 to 2014, he was a Visiting Scholar with the Center for Free-Electron Laser Science (CFEL), Deutsches Elektronen-Synchrotron (DESY), Hamburg, Germany. Since 2015, he has been a Faculty Member with the School of Electrical and Computer Engineering, Shiraz University. His current research interests include microwave photonics and RF/microwaves/millimeter-waves/photonics.



PEDRAM SHOJAADINI received the B.Sc. degree in electrical engineering from the Shahid Bahonar University of Kerman, in 2016, and the M.Sc. degree in electrical engineering from the University of Tehran, Tehran, Iran, in 2019. He is currently pursuing the Ph.D. degree in electrical engineering with the University of Quebec, Gatineau, QC, Canada. His research interests include design, analysis, and development of broadband metasurface and metamaterials. In particular, he studied metasurface absorbers and metasurface energy harvesting.

• • •